Journal of Colloid and Interface Science 327 (2008) 261–265

Contents lists available at ScienceDirect

Journal of Colloid and Interface Science

www.elsevier.com/locate/jcis

Field induced phase segregation in ferrofluids

E.S. Kooij [a,*], A.C. Gâlcă [b], B. Poelsema [a]

[a] Solid State Physics group, MESA+ Institute for Nanotechnology, University of Twente, P.O. Box 217, 7500AE Enschede, The Netherlands
[b] Solid State Magnetism, National Institute of Materials Physics, P.O. Box MG-07, 077125 Magurele, Romania

ARTICLE INFO

Article history:
Received 22 May 2008
Accepted 14 August 2008
Available online 22 August 2008

Keywords:
Magnetic field
Magnetite
Ferrofluid
Interaction

ABSTRACT

We study the phase segregation in magnetite ferrofluids under the influence of an external magnetic field. A phase with lower nanoparticle density and corresponding higher optical transmission is formed in the bottom of a glass cell in the presence of only a very modest magnetic field gradient (smaller than 25 T/m). The flux density in our magnetic configuration is simulated using finite element methods. Upon switching off the external magnetic field, the low-density phase develops into a 'bubble'-like feature. The kinetics of this 'bubble' in the absence and presence of a magnetic field are described and analyzed in terms of a simple model, which takes into account buoyancy and drag forces.

1. Introduction

Magnetic fields provide a powerful, flexible means to control and tune the interactions between magnetic nanoparticles, which are suspended in a solvent. These liquids are also more generally referred to as ferrofluids. The alignment of dipolar entities in a homogeneous field will give rise to net anisotropic interactions between neighboring particles. In an inhomogeneous field, i.e. with a gradient in the magnetic flux density, a net translational force will act on the individual dipolar nanoparticles, enabling assembly of nanoparticles in specific locations, defined by the magnetic field configuration.

With respect to the latter case, field-induced self-assembly of magnetic nanoparticles in suspension and at solid–liquid interfaces has attracted considerable interest over the past decade. A large variety of two- and three-dimensional superstructures of magnetic nanoparticles, assembled using magnetic fields and their gradients, has been reported [1–14]. Magnetophoretic deposition has also been reported as a valuable tool in the fabrication of various nanocomposites. In one example, magnetic nanoparticles are assembled and held on an electrode surface at a predefined density, after which metal atoms are electrochemically deposited in the interstices between them [15]. In another report, a field gradient is used to drive nanoparticles into a polycarbonate membrane to produce granular magnetic nanowires [16]. Recently it has been shown that very low magnetic field gradients can be employed for application in point-of-use water purification and simultaneous separation of complex mixtures [17].

In the absence of a gradient, homogeneous magnetic fields only induce the parallel orientation of the magnetic nanoparticles. As mentioned above this results in highly anisotropic interactions between particles. Interparticle forces are repulsive and attractive in the directions perpendicular and parallel to the applied field, respectively, as clearly observed for example in cryo-TEM images of well-defined suspended magnetic nanoparticles having a permanent dipole moment [13,14]. This effect is well-known and forms the basis of the anisotropic optical properties of ferrofluids subjected to an external field. Since the first discovery of magnetic birefringence and dichroism in these liquids [18,19], substantial research efforts have been focused on elucidating the origin of the magneto-optical properties and exploring their possible application as active optical devices, such as shutters, switches, polarizers and phase-changing elements [20–30].

It is well known that ferrofluids, consisting of dispersed magnetic nanoparticles, exhibit phase separation under the influence of an applied external field [10,31–34]. Labyrinth-like fingering and column-like structures have been observed, which are generally attributed to anisotropic interactions between the nanoparticles in suspensions. For fields parallel to a thin film cell, wire-shaped aggregates of particles align along the field direction. Mutual distances between the wires as well as their lengths can be controlled by the magnetic flux density, the rate of increase of the flux and also the duration of applying the field. Magnetic fields perpendicular to a thin film cell give rise to hexagonally ordered patterns of high-density drop-like aggregates in a low-density matrix. In more theoretical treatments, the phase separation of the ferrofluid with initial concentration into two phases with lower and higher concentrations is generally described in terms of a "ferrocolloidal gas–ferrocolloidal liquid" phase transition.

* Corresponding author.
E-mail address: e.s.kooij@utwente.nl (E.S. Kooij).
URL: http://ssp.tnw.utwente.nl (E.S. Kooij).

0021-9797/$ – see front matter
doi:10.1016/j.jcis.2008.08.029

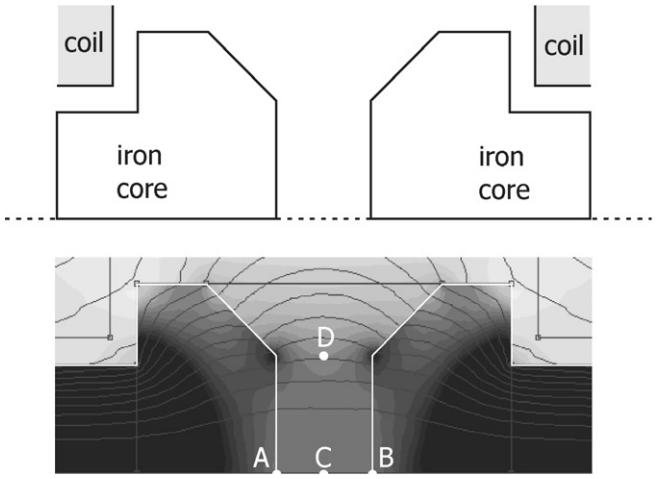

Fig. 1. Two-dimensional axisymmetric representation of the electromagnet configuration used in this work. The distance separating the magnet poles amounts to 18 mm. The corresponding magnetic flux density, shown in the contour plot, was obtained using finite element method calculations. The points A–D are used as reference points, see also Fig. 3.

While performing experiments on the optical birefringence and dichroism of magnetite ferrofluids [30], we obtained some anomalous results, which could not be accounted for by established theories. More specifically, when the (nearly) homogeneous field was applied for long periods of time, typically more than 30 min, irreproducible intensity variations were often observed after switching off the magnetic field. Visual inspection of the system under consideration revealed interesting phenomena, which are most likely related to field-induced phase segregation. In this work, we present our observations, and describe a simple model to account for the results in terms of different phases within the magnetite suspension. The development of a detailed mechanistic model underlying the observed phase segregation is far from straightforward and lies outside the scope of this paper.

2. Experimental observations

For the experiments described in this work, we used a standard electromagnet configuration as schematically shown in Fig. 1. This setup is identical to the one used for the aforementioned magneto-optical studies [30] on diluted magnetite ferrofluids. In the gap between the poles of the magnet, we placed a thin-film glass cell (a standard Starna cuvette) with a 1 mm optical path length, filled with an oil-based magnetite (Fe_3O_4) ferrofluid. Details on sample characteristics, such as preparation conditions, average particle dimension and size distribution have been described elsewhere [30]. The volume fraction of the ferrofluid occupied by magnetite particles ($\Phi_0 = 1.56 \times 10^{-3}$) is considerably smaller than what has previously been considered in studies focused on field-induced phase separation [10,31,33].

In Fig. 2, the glass cell filled with Fe_3O_4 ferrofluid is shown after application of a field of approximately 1 T for 15 min or more. In (a) the field is still applied. On both sides of the cell, the truncated cone-shaped pole-pieces are visible; the width of the gap separating the magnet poles amounts to 18 mm. The magnet axis (the line A–C–B in Fig. 1) is indicated by the white dashed line in Fig. 2. Close examination of Fig. 2a shows that the transmission at the very top of the cell, near the liquid/gas interface, is larger than in the rest of the cell volume. The intensity profile, which in fact visualizes the density of optically absorbing nanoparticles in the suspension, is very similar to the flux density distribution between the poles, as determined from finite element calculations for this specific geometry. The result of these calculations is represented

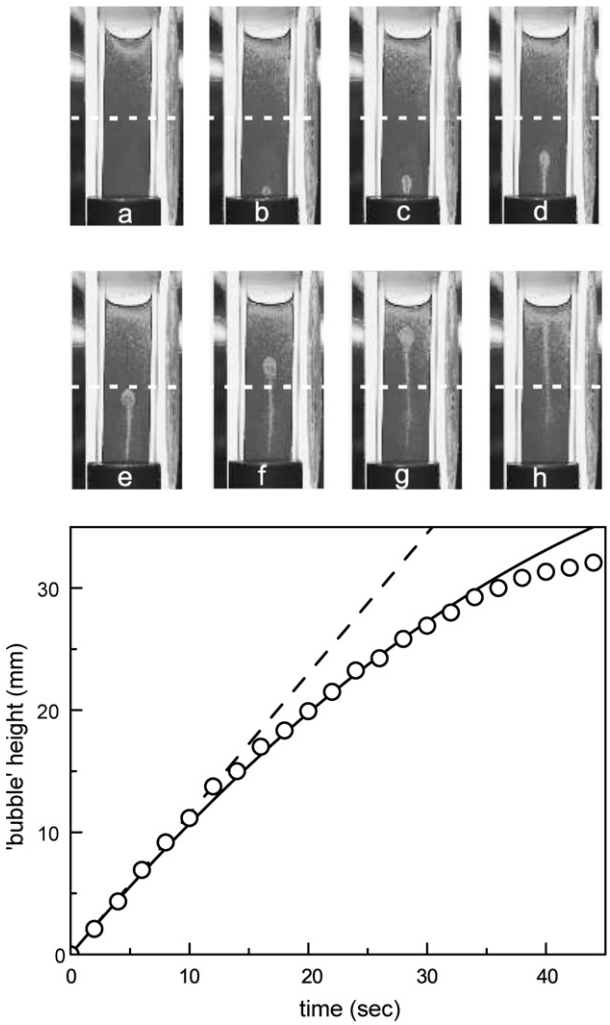

Fig. 2. Series of photographs depicting the field-induced phase separation in a magnetite ferrofluid. The inner width of the glass cell amounts to 10 mm. The applied field is oriented from left to right. The dashed line corresponds to the magnet axis, i.e. the line A–C–B in Fig. 1. The images were recorded (a) at the moment of switching off the magnetic field, (b) after 2 s, (c) 4 s, (d) 8 s, (e) 14 s, (f) 22 s, (g) 32 s, and (h) 44 s. The contrast in the images has been enhanced considerably to visualize relevant features. The height of the low density 'bubble' as a function of time is shown in the graph. The dashed and solid lines are described in the text.

by the contour plot in Fig. 1. The same behavior occurs at the bottom of the glass cell, but since it is inserted into a holder, this is less clearly visible.

Apparently, the small gradient of the slightly inhomogeneous magnetic field at larger distances from the magnet axis (indicated by D in Fig. 1) gives rise to a magnetite nanoparticle density variation within the liquid in the cell. To further clarify this, Fig. 3 shows the flux density variation along high-symmetry direction in the gap between the magnet poles, as obtained from finite element calculations as shown in Fig. 1. Along the magnet axis A–B, the field is very homogeneous with a variation in flux density of less than 3%. In contrast, along the line C–D, precisely in the middle of the gap between the poles, an obvious decrease of the magnetic flux density with increasing distance from the magnet axis, is observed. Most likely, this relatively small gradient, which is smaller than 25 T/m, gives rise to the formation of the low-density ferrofluid phases in the bottom and top of the liquid in the cell. At this time, we have no information on the effect of size distribution on the observed phase segregation. It can be expected that the larger magnetite particles, having a correspondingly larger magnetic moment, are more sensitive to the field gradient as compared

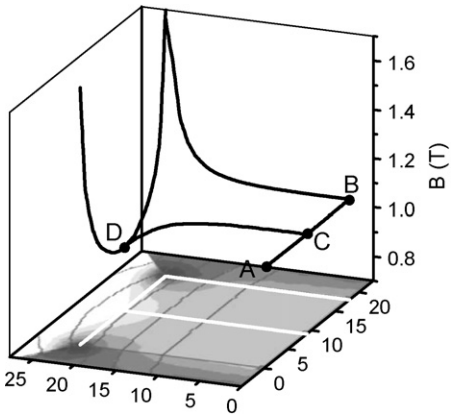

Fig. 3. Three-dimensional representation of the magnetic flux density as obtained from finite element calculations for the magnet configuration in Fig. 1, along high-symmetry directions indicated by A–D. In the *xy*-plane, the contour plot of the flux density in the gap between the poles is shown.

to the smallest entities. As such, the 'darker' high-density phase may contain a relatively larger fraction of magnetite particles with larger dimensions. This is a subject for further investigation in future experiments.

When the magnetic field is switched off, a peculiar flow profile of the ferrofluid is observed in the sequence of images in Figs. 2b–2h. The absence of the magnetic field results in a slight relaxation of the liquid/air interface, as is best seen by comparing Figs. 2a and 2b. Within approximately 2 s, the region with a lower particle density at the bottom of the cell develops into a 'bubble' of low-density phase that starts to rise in the higher density liquid. The nucleation of the 'bubble' is in all cases exactly in the middle between the two poles of the magnet. In Fig. 2 the cell was centered between the magnet poles, so the low-density region is also in the middle of the cell. However, if the cell is displaced from the centered position between the pole pieces by a certain distance, the 'bubble' still originates exactly in the middle of the gap between the poles.

During its ascent, the 'bubble' develops a tail-like feature. Surprisingly, despite considerable convection in the liquid, the two phases (low-density 'bubble' and high-density surrounding liquid) remain reasonably well-separated. Also, the shape of the 'bubble' changes slightly with increasing height, while the 'tail' eventually disappears (see Figs. 2g and 2h at the bottom). The height of the top of the 'bubble' as a function of time is also depicted in the graph in Fig. 2. Apparently, the speed with which the 'bubble' rises toward the surface decreases with increasing height. A more quantitative analysis will be given in the next section.

If the cell is left for sufficient time, typically 5–10 min, diffusion again restores the situation of homogeneously distributed magnetite nanoparticles in the ferrofluid. However, when the magnetic field is again applied during the ascent of the 'bubble,' peculiar behavior is observed. Upon reapplying the field before the 'bubble' reaches the magnet axis, i.e. the middle of the cell, the 'bubble' seems to descend and the density distribution in the liquid is restored very rapidly to the situation prior to switching off the magnetic field.

When the magnetic field is increased after the 'bubble' has passed the middle of the cell, its ascending speed increases markedly (see Fig. 4) and the 'tail' vanishes within seconds, to also yield the original density distribution before switching off the field as shown in Fig. 2a. Apparently, the 'bubble' with lower density ferrofluid phase rushes toward its lowest energetic position, i.e. at the top or bottom of the cell, depending on which of these is at a shorter distance.

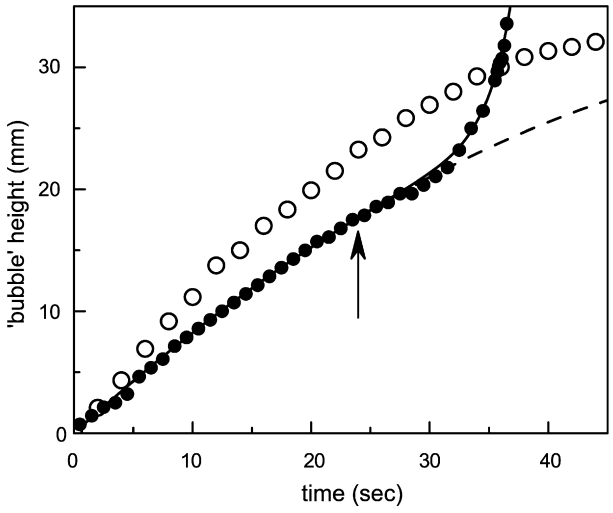

Fig. 4. Height of the 'bubble' as a function of time for two situations. The open circles are identical to the results in Fig. 2. The filled circles show the result of another experiment, in which the field was again applied after 23 s, as indicated by the arrow. The lower initial speed of the 'bubble' in the second experiment reflects the smaller density difference arising from a shorter time during which the initial magnetic field was applied. The dashed and solid lines are discussed in the text.

3. Analysis and discussion

For a quantitative analysis of the experimentally determined height of the 'bubble' as a function of time, as presented in Figs. 2 and 4, we treat the system in a way comparable to the settling of colloidal particles in a gravitational field [35], but in this case it is reversed. If we consider the 'bubble' to be a more or less rigid body, having a lower density due to a lower concentration of magnetite nanoparticles, there are two forces acting upon it. The lower density and thus lower relative weight of the 'bubble' gives rise to a buoyancy force F_{buoy} given by

$$F_{\text{buoy}} = V \cdot \Delta\rho \cdot g, \tag{1}$$

where V is the volume of the 'bubble,' $\Delta\rho = \rho_0 - \rho_1$ is the density difference between the surrounding ferrofluid (ρ_0) and the 'bubble' (ρ_1) and $g = 9.81\ \text{m/s}^2$. This force is obviously directed upwards.

As soon as the 'bubble' starts to move, it will experience a drag force F_{drag} given by [35]

$$F_{\text{drag}} = 6\pi\eta r \cdot u \tag{2}$$

where $\eta = 0.9$ mPa s is the viscosity of the solvent (cyclohexane), r is the effective radius of the 'bubble' and u is its velocity. As mentioned above, the buoyancy force is directed upwards, which implies that the drag force is directed downwards.

Similar to what is assumed for settling colloidal particles, but what is also observed for rising gas bubbles in a liquid, a steady-state situation with a constant velocity u is reached relatively fast. If the ascending velocity is time-independent, the net force on the rising 'bubble' is zero, so Eqs. (1) and (2) are equal. This yields an expression for the density difference

$$\Delta\rho = \frac{6\pi\eta r}{Vg}u. \tag{3}$$

From the initial 'bubble' in Fig. 2c we estimate its radius to amount to approximately $r = 1.05$ mm. The initial velocity amounts to 1.15 mm/s and is indicated by the dashed line in the plot of the height as a function of time in Fig. 2. With the volume $V = 4\pi r^3/3$ and the aforementioned viscosity η, we find that $\Delta\rho = 4.31 \times 10^{-4}\ \text{g/cm}^3$.

The fill fraction $\Phi_0 = 1.56 \times 10^{-3}$ in the ferrofluid used in this study [30] corresponds to a density $\rho_0 = \rho_{\text{cyclo}}(1 - \Phi_0) +$

$\rho_{Fe_3O_4}\Phi_0 = 0.785$ g/cm^3, where $\rho_{cyclo} = 0.779$ g/cm^3 and $\rho_{Fe_3O_4} = 5.10$ g/cm^3 are the densities of cyclohexane and magnetite (Fe_3O_4), respectively. The density difference $\Delta\rho = \rho_0 - \rho_1$ yields a value for the 'bubble' density ρ_1 from which we estimate the fill fraction in the 'bubble' to amount to $\Phi_1 = 1.46 \times 10^{-3}$. From the absorbance spectrum [30] we estimate the initial transmission of the suspension (with $\Phi_0 = 1.56 \times 10^{-3}$) at a wavelength of 650 nm in a cell with an optical path length of 1 mm to amount to 25%. Using the Lambert–Beer law, the lower density and corresponding fill fraction leads to a slightly higher transmission of approximately 28% in the 'bubble'-region; we have to stress that the contrast in the images in Fig. 2 has been enhanced considerably.

As is clearly seen in Fig. 2 the 'bubble' develops a tail-like feature when it rises toward the surface. This implies that its effective volume decreases. Moreover, the 'tail' effectively also reduces the buoyance force acting on the 'bubble.' Additionally, one can consider that due to mixing, induced by convection, the density ρ_1 inside the rising 'bubble' increases with time, i.e. the density difference $\Delta\rho$ between 'bubble' and surrounding, decreases for larger heights. We can take these effects into account by assuming that the velocity decreases linearly with time

$$u(t) = \frac{\Delta\rho \cdot Vg}{6\pi\eta r}(1 - ct). \tag{4}$$

Integration of Eq. (4) and fitting this expression to the data for $t < 30$ s yields the solid line in Fig. 2 and a value for the time-dependence parameter $c = 0.014$. This implies that the buoyancy force decreases by 1.4% of its original value per second, due to an increase of 'bubble' density and/or volume decreases. As can be seen in Fig. 2, the solid line corresponds quite well with the data up to a height of 30 mm. Furthermore, comparing the 'bubble' shape in Fig. 2c to that in Fig. 2f reveals that its effective radius increases for larger heights. This implies that the drag force [Eq. (2)] becomes more pronounced and also slows the ascent of the 'bubble.' Eventually, as it reaches the liquid/gas interface, the 'bubble' will obviously not rise any further but deform and eventually disappear.

Finally, in Fig. 4 we show the result of an experiment in which the field was re-applied as soon as the 'bubble' has passed the center of the magnet configuration (point C in Fig. 1). As described in the previous section, the low-density phase is attracted to the lower magnetic flux density region between the poles, indicated by D in Fig. 3. The slightly lower velocity in the first part of this experiment, as compared to the results in Fig. 2, arises from the shorter time the field was applied prior to $t = 0$ s in the experiment; apparently this gives rise to a smaller density difference $\Delta\rho$ and thus a reduced net force. The dashed line in Fig. 4 is only different from the solid line in Fig. 2 by a constant scaling factor.

To model the acceleration of the 'bubble' we consider the spatial variation of the flux density as presented in Fig. 3, and more specifically along the line C–D. In first approximation, the change of the magnetic flux along the line C–D can be described by an exponential curve. Since the magnetic force is proportional to the spatial derivative of the flux density, the magnetic force exhibits an exponential increase. In Fig. 4 the result of describing the height of the 'bubble' upon again applying the magnetic field at $t = 23$ s as being exponentially time-dependent is shown by the solid line. As can be seen, this very simple model agrees well with the experimentally determined height of the 'bubble' as a function of time.

4. Conclusions

We have investigated the phase segregation in magnetite ferrofluids subjected to very modest magnetic field gradients. The standard electromagnet configuration used in this work has previously been employed to study magneto-optical properties of these ferrofluids. Simulations of the magnetic flux density for this specific configuration using finite element methods reveal that the finite size of the magnet poles results in inhomogeneities in the magnetic field. The magnetite nanoparticle density in the magnetic liquid, as observed by the optical transmission, reflects the magnetic flux distribution. Apparently, magnetic field gradients smaller than 25 T/m are sufficient to induce density differences as observed in this work.

Upon removal of the magnetic field, the liquid phase with lower density in the bottom of the glass cell contracts into a 'bubble'-like feature. This 'bubble' experiences a number of different forces. Most prominently, the difference in ferrofluid density between the 'bubble' and the surrounding liquid results in a buoyancy force directed upwards. As soon as the 'bubble' starts to rise under the influence of this buoyancy force, it will also be subjected to a drag force, which depends on its size. The kinetic behaviour of these phases, as observed by optical video imaging, has been presented and analyzed using a simple model incorporating these forces. We show that such a simple quasi-static equilibrium approximation provides a very good description of the observations.

Finally, once the 'bubble' is moving upwards in the glass cell, the magnetic field can be applied again. Distinctive behaviour is observed which depends on the position of the 'bubble' with respect to the magnetic field gradient. In all cases, the lower density phase is rapidly driven to the location within the magnet configuration with the lowest flux density.

Acknowledgments

We thank A. van Silfhout and F. Mugele for helpful discussions. This work is part of the research program of the Stichting voor Fundamenteel Onderzoek der Materie (FOM), financially supported by the Nederlandse Organisatie voor Wetenschappelijk Onderzoek (NWO).

References

[1] M. Giersig, M. Hilgendorff, J. Phys. D Appl. Phys. 32 (1999) L111–L113.
[2] M. Giersig, M. Hilgendorff, Colloids Surf. A 202 (2002) 207–213.
[3] M. Hilgendorff, B. Tesche, M. Giersig, Aust. J. Chem. 54 (2001) 497–501.
[4] M. Giersig, M. Hilgendorff, Eur. J. Inorg. Chem. 18 (2005) 3571–3583.
[5] A.T. Ngo, M.P. Pileni, Adv. Mater. 12 (2000) 276–279.
[6] M. Spasova, U. Wiedwald, M. Farle, T. Radetic, U. Dahmen, M. Hilgendorff, M. Giersig, J. Magn. Magn. Mater. 272–276 (2004) 1508–1509.
[7] A.T. Ngo, J. Richardi, M.P. Pileni, Langmuir 21 (2005) 10234–10239.
[8] M.P. Pileni, A.T. Ngo, Chem. Phys. Chem. 6 (2005) 1027–1034.
[9] Y. Lalatonne, J. Richardi, M.P. Pileni, Nat. Mater. 3 (2004) 121–125.
[10] H.E. Horng, C.Y. Hong, S.Y. Yang, H.C. Yang, J. Phys. Chem. Solids 62 (2001) 1749–1764.
[11] A. Vorobiev, J. Major, H. Dosch, G. Gordeev, D. Orlova, Phys. Rev. Lett. 93 (2004) 267203.
[12] A. Wiedenmann, U. Keiderling, K. Habicht, M. Russina, R. Gähler, Phys. Rev. Lett. 97 (2006) 057202.
[13] M. Klokkenburg, B.H. Erné, J.D. Meeldijk, A. Wiedenmann, A.V. Petukhov, R. Dullens, A.P. Philipse, Phys. Rev. Lett. 97 (2006) 185702.
[14] M. Klokkenburg, B.H. Erné, A. Wiedenmann, A.V. Petukhov, A.P. Philipse, Phys. Rev. E 75 (2007) 051408.
[15] J.L. Katz, Y. Xing, R.C. Cammarata, J. Mater. Res. 14 (1999) 4457–4459.
[16] J.E. Wegrowe, T. Wade, X. Hoffer, L. Gravier, J.M. Bonard, J.P. Ansermet, Phys. Rev. B 67 (2003) 104418.
[17] C.T. Yavuz, J.T. Mayo, W.W. Yu, A. Prakash, J.C. Falkner, S. Yean, L. Cong, H.J. Shipley, A. Kan, M. Tomson, D. Natelson, V.L. Colvin, Science 314 (2006) 964.
[18] Q. Majorana, C.R. Hebd. Acad. Sci. 135 (1902) 235–237.
[19] A. Cotton, H. Mouton, C.R. Hebd. Acad. Sci. 141 (1905) 317–319.
[20] H.W. Davies, J.P. Llewellyn, J. Phys. D Appl. Phys. 13 (1980) 2327–2336.
[21] P.C. Scholten, J. Phys. D Appl. Phys. 13 (1980) L231–L234.
[22] J.P. Llewellyn, J. Phys. D Appl. Phys. 16 (1983) 95–104.
[23] S. Taketomi, Jpn. J. Appl. Phys. 22 (1983) 1137–1143.
[24] M. Xu, P.J. Ridler, J. Appl. Phys. 82 (1997) 326–332.
[25] E. Hasmonay, E. Dubois, J.-C. Bacri, R. Perzynski, Y. Raikher, V. Stepanov, Eur. Phys. J. B 5 (1998) 859–867.

[26] H.E. Horng, C.-Y. Hong, H.C. Yang, I.J. Jang, S.Y. Yang, J.M. Wu, S.L. Lee, F.C. Kuo, J. Magn. Magn. Mater. 201 (1999) 215–217.
[27] M. Rasa, Eur. Phys. J. E 2 (2000) 265–275.
[28] E. Hasmonay, J. Depeyrot, M.H. Sousa, F.A. Tourinho, J.-C. Bacri, R. Perzynski, Y.L. Raikher, I. Rosenman, J. Appl. Phys. 88 (2000) 6628–6635.
[29] V. Socoliuc, D. Bica, J. Magn. Magn. Mater. 289 (2005) 177–180.
[30] E.S. Kooij, A.C. Galca, B. Poelsema, J. Colloid Interface Sci. 304 (2006) 261.
[31] H. Wang, Y. Zhu, C. Boyd, W. Luo, A. Cebers, R.E. Rosenschweig, Phys. Rev. Lett. 72 (1994) 1929.
[32] Y.A. Buyevisch, A.O. Ivanov, Physica A 190 (1992) 276–294.
[33] C.Y. Hong, I.J. Jang, H.E. Horng, C.J. Hsu, Y.D. Yao, H.C. Yang, J. Appl. Phys. 81 (1997) 4275–4277.
[34] A.O. Ivanov, A.Y. Zubarev, J. Magn. Magn. Mater. 201 (1999) 222–225.
[35] R.J. Hunter, Foundations of Colloid Science, Oxford Univ. Press, New York, 2001.